IEEE Photonics Journal
An IEEE Photonics Society Publication

Tunable Electromagnetically Induced Transparency in Plasmonic System and Its Application in Nanosensor and Spectral Splitting

Volume 7, Number 6, December 2015

Zhao Chen
Xiaokang Song
Rongzhen Jiao
Gaoyan Duan
Lulu Wang
Li Yu

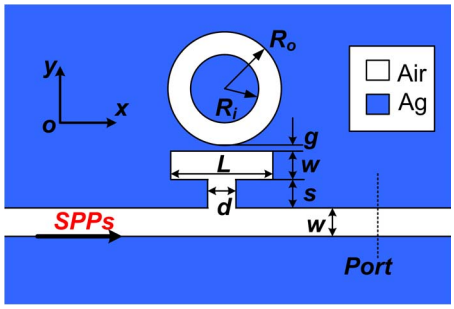

DOI: 10.1109/JPHOT.2015.2492550
1943-0655

Tunable Electromagnetically Induced Transparency in Plasmonic System and Its Application in Nanosensor and Spectral Splitting

Zhao Chen, Xiaokang Song, Rongzhen Jiao, Gaoyan Duan, Lulu Wang, and Li Yu

State Key Laboratory of Information Photonics and Optical Communications, Beijing University of Posts and Telecommunications, Beijing 100876, China
School of Science, Beijing University of Posts and Telecommunications, Beijing 100876, China

DOI: 10.1109/JPHOT.2015.2492550

Manuscript received September 28, 2015; revised October 10, 2015; accepted October 15, 2015. Date of publication October 26, 2015; date of current version October 30, 2015. This work was supported in part by the National Natural Science Foundation of China under Grant 11374041, Grant 11404030, Grant 61571060, and Grant 11574035 and in part by the Fund of State Key Laboratory of Information Photonics and Optical Communications, Beijing University of Posts and Telecommunications, Beijing, China. Corresponding author: L. Yu (e-mail: bupt.yuli@gmail.com).

Abstract: A compact structure is proposed to achieve electromagnetically induced transparency (EIT) response, which consists of a side-coupled cavity and a ring resonator. Novel structures and the transmission characteristics are studied in several different situations. The plasmonic device can be used as a high-sensitivity refractive sensor with a sensitivity of 1200 nm/RIU. In addition, multi-EIT-like peaks appear in the original broadband spectrum by adding another side-coupled cavity or ring resonator, and the physical mechanism is presented. The system paves a new way toward highly integrated optical circuits and networks, particularly for nanosensor, spectral splitter, and nonlinear devices.

Index Terms: Surface plasmons, electromagnetically induced transparency (EIT), meatl-insulator-metal (MIM) waveguide, nanosensor, spectral splitting.

1. Introduction

Surface plasmon polaritons (SPPs) are considered to have dramatically potential application in realization of highly integrated optical circuits due to their capability to overcome the diffraction limit of light [1]. To date, various types of plasmonic devices have been demonstrated experimentally and simulated numerically [2], [3]. For example, Chai *et al.* experimentally realized ultracompact chip-integrated electromagnetically induced transparency (EIT) in a single plasmonic composite nanocavity [4]. Wang *et al.* proposed a graded non-linear plasmonic grating to realize all-optical switch [5]. As an intriguing physical phenomenon, EIT occurs in atomic systems due to the quantum destructive interference between the excitation pathways to the atomic upper level [6], [7]. Tremendous attention has been attracted to study EIT phenomenon and they have been observed in various plasmonic structures, such as symmetry-reduced grating structure [8], coupled resonant systems [9], [10], metamaterials [11]–[13] and metal-insulator-metal (MIM) waveguides [14]–[17]. Among all the nanostructures, the MIM waveguide structures have attracted many researchers' attention due to their deep-sub-wavelength confinement of

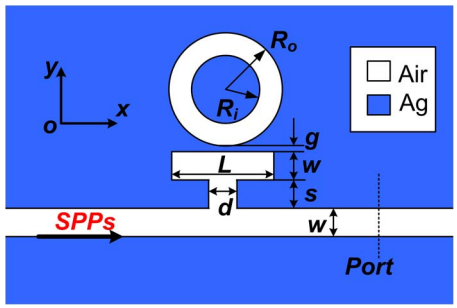

Fig. 1. Schematic configuration and geometric parameters of the plasmonic waveguide system.

light [18]–[21]. These structures are more suitable for the highly integrated optical circuits. Thus, the MIM waveguide has wide applications in deep subwavelength optical devices, such as filters [22], [23], sensors [24], [25] and demultiplexers [26]–[28]. These results may open up a pathway in photonics and offer prospects of smaller devices for the manipulation and transmission of light. Therefore, combining the EIT-like response with MIM waveguide structures would create the possibility of achieving ultracompact functional optical components for use in highly integrated optics [11].

In this paper, a compact plasmonic waveguide coupled with a side-coupled cavity and a ring resonator is proposed to generate EIT-like response. Simulation results show that the transparency windows can be easily tuned by changing the parameters of the structure and the material imbedded in the ring resonator. The proposed structure can serve as an excellent plasmonic sensor with a sensitivity of $\sim$1200 nm/RIU. In addition, the spectrum can be effectively split by expanding the original structure by means of adding another side-coupled cavity or ring resonator. These results could be applied for developing ultra-compact plasmonic devices in highly all-optical integration systems.

2. Theory and Model

The plasmonic nanostructure is shown in Fig. 1, which consists of a MIM waveguide with a side-coupled cavity and a ring resonator. The width and length of the side-coupled cavity is w and L, the outer and inner radius of the ring is R_o and R_i, respectively. The width of the bus waveguide is w, and g denotes the coupling distance between the side-couple cavity and the ring resonator. This system is a two-dimensional model, and the blue and white parts signify the Ag (ε_m) and air $(\varepsilon_d = 1.0)$, respectively. The presence of the aperture, width d and height s, is to ensure a strong coupling between the side-coupled cavity and the bus waveguide [29]. Herein, w, d, s and $R_o - R_i$ are fixed to be 50 nm throughout this letter. When the SPPs waves propagate forward along the bus waveguide, most of them will be coupled to the side-coupled cavity through the aperture, then it could be partly coupled to the ring resonator. The transmittance of the SPPs is defined as the quotient between the SPP power flows (obtained by integrating the Poynting vector over the channel cross section) of the observing port with structures (aperture, side-coupled cavity and ring resonator) and without structures [30], [31]. Since the width of the bus guide is much smaller than the incident light, only a single propagation mode TM_0 can exist in the structure, whose dispersion relation is determined by the equation [32]

$$\varepsilon_d\sqrt{\beta_{spp}^2-\varepsilon_m k_0^2}+\varepsilon_m\sqrt{\beta_{spp}^2-\varepsilon_d k_0^2}\,\tanh\left(w\sqrt{\beta_{spp}^2-\varepsilon_d k_0^2}/2\right)=0 \tag{1}$$

where $k_0 = 2\pi/\lambda$ is the free-space wave vector, and β_{spp} is the wave vector of SPPs in the MIM waveguide. The permittivity of silver is characterized by the well-known Drude model [21]:

$$\varepsilon_m = \varepsilon_\infty - \frac{\omega_p^2}{\omega^2 + i\omega\gamma}. \tag{2}$$

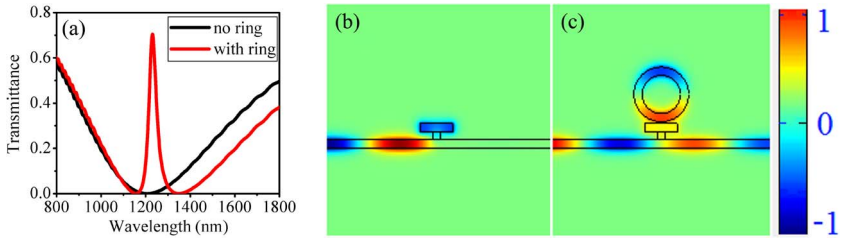

Fig. 2. (a) Transmission spectra without (black line) and with (red line) the ring of the proposed structure. (b), (c) H_z field distributions without and with the ring at $\lambda = 1232$ nm.

Here, $\varepsilon_\infty = 3.7$, $\omega_p = 9.1$ eV, and $\gamma = 0.018$ eV, which fits the experiment optical constant of silver [33] for the range of 800$\sim$2000 nm quite well.

Based on the standing wave theory [34], the resonant wavelength is determined by the resonance condition:

$$\lambda = \frac{2n_{eff}L_{eff}}{m}. \tag{3}$$

Here, L_{eff} is the effective length of the resonator; n_{eff} is the effective refraction index of SPPs, which can be written as $n_{eff} = \beta_{spp}/k_0$; and m is a positive integer, which represents the order of resonance. Based on (3), we can obtain that the dependence of the variation of the resonant wavelength on the resonator length L_{eff} is

$$\frac{d\lambda}{dL_{eff}} = \frac{2n_{eff}}{m}. \tag{4}$$

3. Simulations and Results

The properties of the proposed structure are investigated using the finite element method (FEM) with Comsol Multiphysics. In the simulations, the parameters are set to be $L = 200$ nm, $g = 10$ nm, $R_i = 115$ nm, and $R_o = 165$ nm. Fig. 2(a) shows the transmission spectra without and with the ring resonator. It is found that the transmission spectrum exhibits a broad dip at $\lambda = 1232$ nm, when the ring resonator is removed. While when the ring resonator is added up the side-coupled cavity, a narrow transmission peak emerges in the original broad dip. This is a typical EIT-like spectral response [6], [15], [21], which originates from the interaction between the broad continuous spectrum and the narrow discrete resonance caused by the side-coupled cavity and the ring resonator, respectively. At the resonant wavelength $\lambda = 1232$ nm, calculations show that the effective refractive index and the propagation length of the SPPs in this MIM waveguide are $n_{eff} = 1.38 - 0.003$ i and $L_{SPP} = 32.7$ μm, respectively (by solving the eigenfunction [Eq. (1)] of the SPP wave vector in the MIM waveguide). In the simulations, the proposed structure (see Fig. 1) is very compact (total length about 2 μm), which is much smaller than the propagation length (about 32.7 μm) of SPPs, so the Ohmic loss in the metal can be neglected. The corresponding field H_z distributions at the transparency window without and with the ring resonator are displayed in Fig. 2(b) and (c), respectively. It can be seen from Fig. 2(b) that the energy of the incident wave is stored in the side-coupled cavity. However, the energy in the side-coupled cavity transfers to the ring resonator due to the destructive interference between the two resonators, as shown in Fig. 2(c). Therefore, we can know that the main behavior of the transparency window is determined by the ring resonator.

As we know, the transmission characteristics of the plasmonic waveguide systems can be affected by the structure parameters. First, we calculated the transmission spectra for different radius R_o with $L = 200$ nm, as shown in Fig. 3(a). It is found that the resonance peak has a red shift with a slope of $\Delta\lambda/\Delta R_o \approx 8.667$, as shown in the black dashed line in Fig. 3(a). In this case, the effective length of the resonator is $L_{eff} = 2\pi(R_o + R_i)/2 = \pi(R_o + R_i)$, thus based on (4), it is easy to get that $d\lambda/dR_o = 2n_{eff} \times \pi(1 + R_i/R_o)/m = 2 \times 1.38 \times \pi(1 + R_i/R_o)/2 \approx 8.671$.

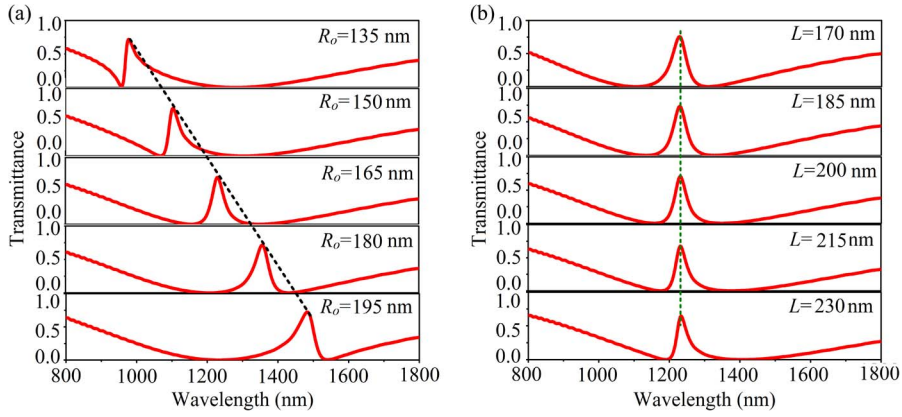

Fig. 3. (a) Transmission spectra for different radius of the ring resonator with $L = 200$ nm. (b) Transmission spectra for different length of the side-coupled cavity with $R_o = 165$ nm.

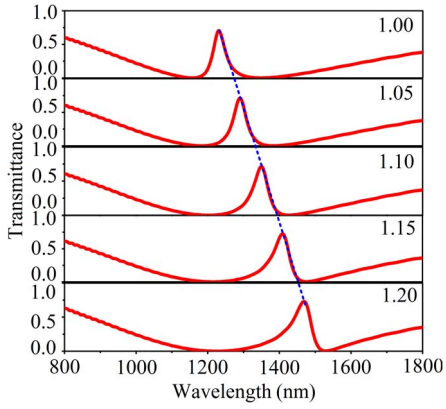

Fig. 4. Transmission spectra for different refractive index with $L = 200$ nm and $R_o = 165$ nm.

These results agree well with the slope of the black dashed line in Fig. 3(a). According to the simulation results, the EIT-like peaks can be easily manipulated by adjusting the radius of the ring resonator.

Successively, we investigated the influence of the length of the side-coupled cavity L on the transparency windows when $R_o = 165$ nm, and as shown in Fig. 3(b). It is clearly that the transparency windows keep almost unchanged $(\Delta\lambda/\Delta L \approx 0)$ with L increasing or a fixed R_o, as shown the green dashed line in Fig. 3(b). Because the resonant wavelength of the EIT-like is determined by the ring resonator [see Fig. 2(c)].

4. Sensing Applications Based on EIT

Compact and light-weight diagnostic devices hold significant promise for early detection and monitoring of diseases in field settings. Plasmonic nanosensors are one of the key components [25], [31], [35]. Therefore, the influence of the material embedded in the ring resonator on the transparency windows is studied, as shown in Fig. 4. It is obvious that the transparency windows redshift with a slope $\Delta\lambda/\Delta n \approx 1200$. According to (4), we can get $d\lambda/dn = 2n_{eff} \times \pi(R_o + R_i)/m = 2 \times 1.38 \times \pi(165 + 115)/2 \approx 1214$, agreeing well with the slope of the blue dashed line in Fig. 4. This feature provides an excellent scheme for the applications toward nanoscale sensing [36]. The sensitivity of a sensor (nm/RIU) is usually defined as the shift in the resonance wavelength per unit variations of the refractive index [37]. Thus, the sensitivity of

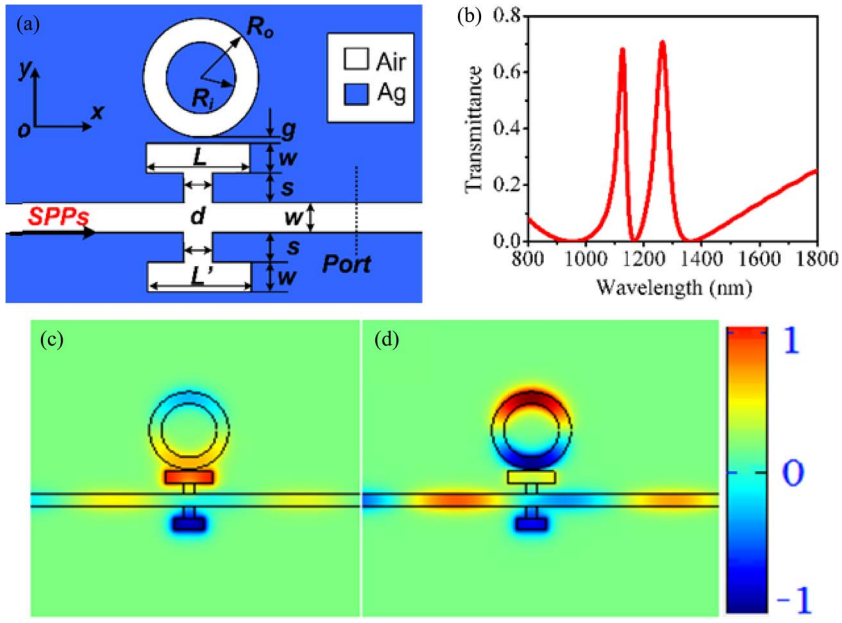

Fig. 5. (a) Schematic configuration and geometric parameters of double side-coupled cavities and one ring resonator. (b) Transmission spectrum of the system with $R_o = 165$ nm, $L = 200$ nm, and $L' = 125$ nm.

the proposed structure is 1200 nm/RIU. These results are higher than that (588 nm/RIU) in the reference [36] due to the strongly resonance in the ring resonator.

5. Spectral Splitting Based on EIT

The proposed EIT structure is flexible and can be easily extended to a double EIT system by adding a side-coupled cavity, as shown in Fig. 5(a). Fig. 5(b) shows the transmission spectrum of the new structure. It is obvious that a new transmission peak emerges, revealing double EIT-like optical response. The corresponding field distributions of H_z at the two peaks are displayed in Fig. 5(c) and (d). From Fig. 5(c) $(\lambda = 1127$ nm$)$, we know that the energy is almost confined in the two side-coupled cavities, which has different length. The SPPs reflected back and forth between the upper and lower cavities, constructing a Fabry–Pérot resonator [2], indicating that the new emerging peak is mainly due to the interaction between the two side-coupled cavities. Comparing with Figs. 2(c) and 5(d), we know that they have similar field distribution. Therefore, the low energy EIT peak or $\lambda = 1265$ nm is caused by the coupling between the side-coupled cavity and the ring resonator.

In addition, another plasmonic structure is also proposed to achieve double EIT-like transmission spectrum, as shown in Fig. 6. The structure system consists of one side-coupled cavities and two ring resonator. The coupling distance between the two ring resonators is also denoted as g $(g = 10$ nm$)$. Numerical simulation shows that only the radius of the two ring resonators are equivalent ($R_o = R_o'$, $R_i = R_i'$) that the two peaks can reach the highest. The FEM is used to calculate the transmission properties with different materials imbedded in the ring resonators, which are displayed in Fig. 7(a)–(e). Obviously, two EIT peaks emerge in the wide transmission spectra. The corresponding field distributions H_z at these two EIT peaks are displayed in Fig. 7(f) and (g). This phenomenon is similar to the mode splitting according to the plasmon hybridization theory, which is used in the coupled metal nanoparticle systems [38]. From Fig. 7(f) and (g), we can see that the side-coupled cavity resonates weakly while the two ring resonators resonate strongly, which is similar to the single EIT system shown in Fig. 1. The difference between the two EIT peaks is that the phase of H_z in the adjacent of the two

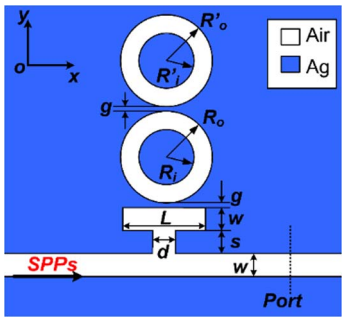

Fig. 6. Schematic configuration and geometric parameters of one side-coupled cavities and two ring resonator.

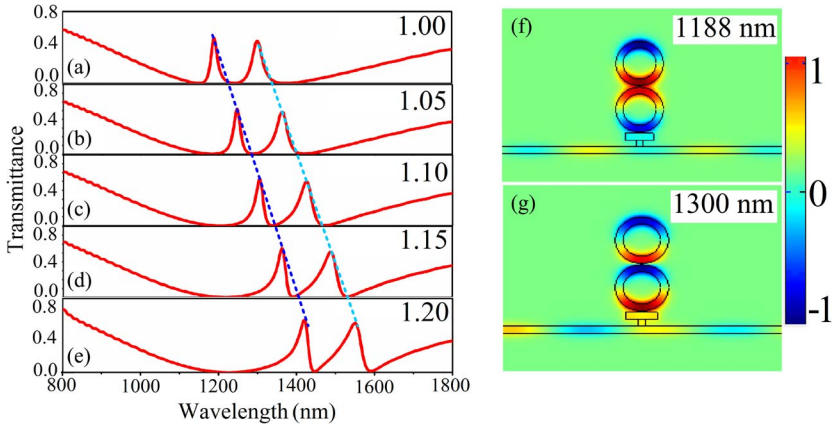

Fig. 7. (a)–(e) Transmission spectra for different refractive index. Field distributions H_z at (f) $\lambda = 1188$ nm and (g) $\lambda = 1300$ nm when $n = 1.00$. Parameters are set as $L = 200$ nm, $R_o = R'_o = 165$ nm, and $R_i = R'_i = 115$ nm.

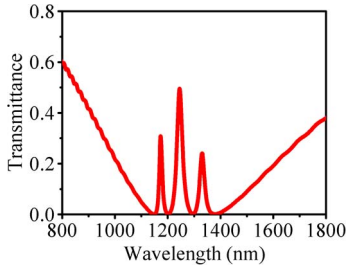

Fig. 8. Transmission spectrum of the system with three ring resonators and one side-coupled cavity.

ring resonators are inphase and antiphase for the high energy EIT peak ($\lambda = 1188$ nm) and low energy EIT peak ($\lambda = 1300$ nm), respectively. According to the above results, the resonance spectra are split because of the phase-coupled effects. Moreover, the two EIT-like peaks are both varies linearly with the refractive index, as shown the blue and green dashed lines in Fig. 7. These characteristics also offer flexibility to design a plasmonic nanosensor. This nanosensor yields a sensitivity of ~1200 nm/RIU. Although the sensitivity of nanosensor does not improve, this structure can be served as a better spectral splitter.

Based on above analysis, the structure (not shown here) with third ring resonator, which placed above the second ring resonator, is investigated to achieve three spectral splitting. Fig. 8

shows the transmission spectrum of the system. Herein, the three ring resonators have the same radius ($R_o = 165$ nm, $R_i = 115$ nm). It is obvious that three narrower EIT-like peaks occur in the broadband transmission spectrum. The multi-resonator-coupled system with multi-EIT-like optical responses may have complex functional applications, such as channel selection, channel add-drop, multichannel switches, and wavelength-division multiplexing.

6. Conclusion

In conclusion, a novel plasmonic structure, which is composed of a side-coupled cavity and a ring resonator, is proposed and its transmission properties are investigated by FEM. Simulation results show that a typical EIT-like response emerges in the original broad dip, and the it can be easily tuned by changing the parameters of the structure and the material imbedded in the ring resonator. Based on above analysis, a nanosensor with a sensitivity 1200 nm/RIU and spectral splitter are achieved. Our structures may have important potential applications in highly integrated optical circuits and networks, especially for the nanosensor, spectral splitter, and nonlinear devices.

References

[1] W. L. Barnes, A. Dereux, and T. W. Ebbesen, "Surface plasmon subwavelength optics," *Nature*, vol. 424, no. 6950, pp. 824–830, Aug. 2003.
[2] J. Chen, Z. Li, S. Yue, J. Xiao, and Q. Gong, "Plasmon-induced transparency in asymmetric T-shape single slit," *Nano Lett.*, vol. 12, no. 5, pp. 2494–2498, May 2012.
[3] V. F. Nezhad, S. Abaslou, and M. S. Abrishamian, "Plasmonic band-stop filter with asymmetric rectangular ring for WDM networks," *J. Opt.*, vol. 15, no. 5, Apr. 2013, Art. ID. 055007.
[4] Z. Chai *et al.*, "Ultracompact chip-integrated electromagnetically induced transparency in a single plasmonic composite nanocavity," *Adv. Opt. Mater*, vol. 2, no. 4, pp. 320–324, Apr. 2014.
[5] G. Wang, H. Lu, X. Liu, and Y. Gong, "Numerical investigation of an all-optical switch in a graded nonlinear plasmonic grating," *Nanotech.*, vol. 23, no. 44, Oct. 2012, Art. ID. 444009.
[6] Q. Xu *et al.*, "Experimental realization of an on-chip all-optical analogue to electromagnetically induced transparency," *Phy. Rev. Lett.*, vol. 96, no. 12, Mar. 2006, Art. ID. 123901.
[7] M. Fleischhauer, A. Imamoglu, and J. P. Marangos, "Electromagnetically induced transparency: Optics in coherent media," *Rev. Mod. Phys.*, vol. 77, no. 2, pp. 633–673, Jul. 2005.
[8] Z. Dong, P. Ni, J. Zhu, and X. Zhang, "Transparency window for the absorptive dipole resonance in a symmetry-reduced grating structure," *Opt. Exp.*, vol. 20, no. 7, pp. 7206–7211, Mar. 2012.
[9] X. Zhou *et al.*, "Phase characteristics of an electromagnetically induced transparency analogue in coupled resonant systems," *New J. Phy.*, vol. 15, Jun. 2013, Art. ID. 103033.
[10] A. Artar, A. Yanik, and H. Altug, "Multispectral plasmon induced transparency in coupled meta-atoms," *Nano Lett.*, vol. 11, pp. 1685–1689, Mar. 2011.
[11] N. Liu *et al.*, "Plasmonic analogue of electromagnetically induced transparency at the Drude damping limit," *Nature Mater.*, vol. 8, pp. 758–762, Sep. 2009.
[12] J. Gu *et al.*, "Active control of electromagnetically induced transparency analogue in terahertz metamaterials," *Nature Commun.*, vol. 3, Oct. 2012, Art. ID. 1151.
[13] X. Jin *et al.*, "Highly-dispersive transparency at optical frequencies in planar metamaterials based on two-bright-mode coupling," *Opt. Exp.*, vol. 19, no. 22, pp. 21652–21657, Oct. 2011.
[14] Z. Han and S. Bozhevolnyi, "Plasmon-induced transparency with detuned ultracompact Fabry–Pérot resonators in integrated plasmonic devices," *Opt. Exp.*, vol. 19, no. 4, pp. 3251–3257, Feb. 2011.
[15] J. Chen, C. Wang, R. Zhang, and J. Xiao, "Multiple plasmon-induced transparencies in coupled-resonator systems," *Opt. Lett.*, vol. 37, no. 24, pp. 5133–5135, Dec. 2012.
[16] H. Lu, X. Liu, G. Wang, and D. Mao, "Tunable high-channel-count bandpass plasmonic filters based on an analogue of electromagnetically induced transparency," *Nanotech.*, vol. 23, no. 44, Oct. 2012, Art. ID. 444003.
[17] K. Wen *et al.*, "Electromagnetically induced transparency-like transmission in a compact side-coupled T-shaped resonator," *J. Lightwave Technol.*, vol. 32, no. 9, pp. 1701–1707, May 2014.
[18] Z. Chen, L. Cui, X. Song, L. Yu, and J. Xiao, "High sensitivity plasmonic sensing based on Fano interference in a rectangular ring waveguide," *Opt. Commun.*, vol. 340, pp. 1–4, Nov. 2014.
[19] J. J. Chen *et al.*, "Response line-shapes in compact coupled plasmonic resonator systems," *Plasmonics*, vol. 8, no. 2, pp. 1129–1134, Jun. 2013.
[20] G. Zheng *et al.*, "Band-stop filters based on a coupled circular ring metal-insulator-metal resonator containing nonlinear material," *J. Opt.*, vol. 14, no. 5, Mar. 2012, Art. ID. 055001.
[21] H. Lu, X. Liu, D. Mao, Y. Gong, and G. Wang, "Induced transparency in nanoscale plasmonic resonator systems," *Opt. Lett.*, vol. 36, no. 16, pp. 3233–3235, Aug. 2011.
[22] H. Zhang, D. Shen, and Y. Zhang, "Circular split-ring core resonators used in nanoscale metal-insulator-metal band-stop filters," *Laser Phys. Lett.*, vol. 11, Oct. 2014, Art. ID. 115902.

[23] J. Chen *et al.*, "Tunable resonances in the plasmonic split-ring resonator," *IEEE Photon. J.*, vol. 6, no. 3, Jun. 2014, Art. ID. 4800706.
[24] J. J. Chen *et al.*, "Coupled-resonator-induced Fano resonances for plasmonic sensing with ultra-high figure of merits," *Plasmonics*, vol. 8, no. 4, pp. 1627–1632, Dec. 2013.
[25] H. Lu, X. M. Liu, D. Mao, and G. X. Wang, "Plasmonic nanosensor based on Fano resonance in waveguide-coupled resonators," *Opt. Lett.*, vol. 37, no. 18, pp. 3780–3782, Sep. 2012.
[26] J. J. Chen, Z. Li, J. Li, and Q. H. Gong, "Compact and high-resolution plasmonic wavelength demultiplexers based on Fano interference," *Opt. Exp.*, vol. 19, no. 10, pp. 9976–9985, May 2011.
[27] G. X. Wang, H. Lu, X. M. Liu, D. Mao, and L. N. Duan, "Tunable multi-channel wavelength demultiplexer based on MIM plasmonic nanodisk resonators at telecommunication regime," *Opt. Exp.*, vol. 19, no. 4, pp. 3513–3518, Feb. 2011.
[28] A. Noual, A. Akjouj, Y. Pennec, J. Gillet, and B. Djafari-Rouhani, "Modeling of two-dimensional nanoscale Y-bent plasmonic waveguides with cavities for demultiplexing of the telecommunication wavelengths," *New J. Phys.*, vol. 11, no. 10, Oct. 2009, Art. ID. 103020.
[29] Z. Han, V. Van, W. N. Herman, and P. Ho, "Aperture-coupled MIM plasmonic ring resonators with sub-diffraction modal volumes," *Opt. Exp.*, vol. 17, no. 15, pp. 12678–12684, Jul. 2009.
[30] Z. Chen, J. J. Chen, L. Yu, and J. H. Xiao, "Sharp trapped resonances by exciting the anti-symmetric waveguide mode in a metal-insulator-metal resonator," *Plasmonic*, vol. 10, no. 1, pp. 131–137, Feb. 2015.
[31] Z. Chen and L. Yu, "Multiple Fano resonances based on different waveguide modes in a symmetry breaking plasmonic system," *IEEE Photon. J.*, vol. 6, no. 6, Nov. 2014, Art. ID. 4802208.
[32] J. Dionne, L. Sweatlock, and H. Atwater, "Plasmon slot waveguides: Towards chip-scale propagation with subwavelength-scale localization," *Phys. Rev. B*, vol. 73, no. 3, Jan. 2006, Art. ID. 035407.
[33] P. B. Johnson and R. W. Christy, "Optical constants of the noble metals," *Phys. Rev. B*, vol. 6, no. 12, pp. 4370–4379, Dec. 1972.
[34] Z. P. Zhou, F. F. Hu, and H. X. Yi, "Wavelength demultiplexing structure based on arrayed plasmonic slot cavities," *Opt. Lett*, vol. 36, no. 8, pp. 1500–1502, Apr. 2011.
[35] K. Mayer and J. Hafner, "Localized surface plasmon resonance sensors," *Chem. Rev.*, vol. 111, no. 6, pp. 3828–3857, Jun. 2011.
[36] N. Liu *et al.*, "Planar metamaterial analogue of electromagnetically induced transparency for plasmonic sensing," *Nano Lett.*, vol. 10, no. 4, pp. 1103–1107, Apr. 2010.
[37] N. Liu, M. Mesch, T. Weiss, M. Hentschel, and H. Giessen, "Infrared perfect absorber and its application as plasmonic sensor," *Nano Lett.*, vol. 10, no. 7, pp. 2342–2348, Jun. 2010.
[38] P. Nordlander and C. Oubre, "Plasmon hybridization in nanoparticle dimers," *Nano Lett.*, vol. 4, no. 5, pp. 899–903, Mar. 2004.